New inferences of mantle viscosity from joint inversion of long-wavelength mantle convection and post-glacial rebound data

Alessandro M. Forte

Institut de Physique du Globe de Paris, Dépt. de Sismologie, Paris, France

Jerry X. Mitrovica

Department of Physics, University of Toronto, Toronto, Ontario, Canada

Abstract.

We perform joint inversions for mantle viscosity of geophysical observables associated with both mantle convection and glacial isostatic adjustment (GIA). Our data include coefficients of the non–hydrostatic geoid (up to degree 8) and decay times associated with post-glacial relative sea level (RSL) variations in Hudson Bay and Fennoscandia. We find that both data sets may be reconciled using a single profile of mantle viscosity which is characterized by a significant increase, with depth, across this region. This result weakens previous arguments that the mantle rheology has significant transient effects. The viscosity profiles we obtain are found to reconcile the observed free air gravity anomaly over Hudson Bay.

Introduction

Historically, in situ inferences of mantle viscosity have been derived from geophysical signatures associated with either GIA [e.g., *Haskell*, 1935] or the mantle convection circulation [e.g., *Hager*, 1984; *Richards and Hager*, 1984]. An early indication that the inferences from the two data sets may be contradictory, with the convection signatures suggesting a much larger increase in viscosity, with depth, than that preferred on the basis of the GIA data set, motivated the study of transient effects in the mantle rheology [e.g., *Sabadini et. al*, 1985; *Peltier*, 1985]. The necessity of invoking transient rheology has been weakened by recent studies which suggest that a number of GIA data sets are consistent with a large viscosity increase from the upper to lower mantle [e.g., *Nakada and Lambeck*, 1989]. Furthermore, *Mitrovica* [1996] has demonstrated that past GIA analyses have commonly misinterpreted the classic *Haskell* [1935] value of 10^{21} Pa s as a constraint on the average viscosity down to 670 km depth (the constraint actually extends to ~ 1400 km depth), and that this may have biased some previous inferences toward near isoviscous profiles. *Mitrovica* [1996] has also sug-

gested that the insensitivity of most RSL variations due to GIA to the viscosity in the bottom half of the lower mantle (below 1800 km depth) may permit a reconciliation of inferences based on GIA data and the long-wavelength signatures of mantle convection. In this paper we address the issue of reconciliation by performing a joint inversion of data associated with convectively supported long–wavelength gravity anomalies and post-glacial RSL variations.

GIA on a Maxwell Viscoelastic Planet

RSL curves for sites near the center of previously glaciated regions commonly exhibit simple exponential variations. A model for this trend is:

$$RSL_i(t) = A_i\{exp(t/\tau_i) - 1\}, \qquad (1)$$

where the subscript i denotes the ith geographic site, and t is time measured into the past. *Mitrovica and Peltier* [1995] and *Mitrovica* [1996] have demonstrated that decay times τ_i estimated from the post-glacial uplift of some sites provide constraints on mantle viscosity which are relatively insensitive to uncertainties in the ice load history. In the analysis below we adopt this decay time parameterization.

We will consider post–glacial RSL variations at two sites: Richmond Gulf (RG) and Angerman River (AR). Richmond Gulf is located in southern Hudson Bay, near the centre of the former Laurentide ice complex. Angerman River, adjacent to the Gulf of Bothnia, is located near the centre of the ancient Fennoscandian ice complex. The RSL curves for these sites are believed to be amongst the most accurate from these regions (see *Mitrovica* [1996]). Following *Mitrovica* [1996], we adopt a 9.0 kyr time window for the Angerman River site and a 6.5 kyr time window for Richmond Gulf. These values ensure that the post-glacial RSL variation at each location is dominated by a free-decay adjustment. A Monte–Carlo procedure is used to find the best-fitting form (1) through the data at each site, while a least-squares estimate starting at this solution yields the observational uncertainty in the decay times (Fig. 1).

Our forward RSL predictions are based on the response of spherically symmetric, self-gravitating, Maxwell visco–elastic Earth models to a prescribed ice load-
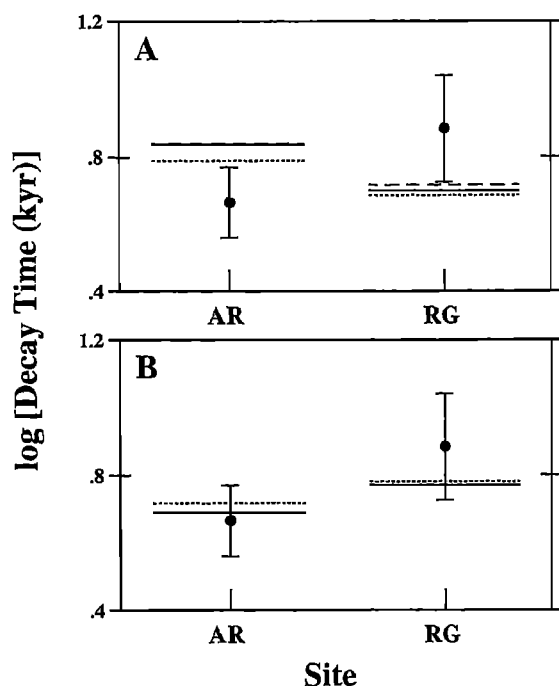
Fig. 1. (A) Numerical predictions of post-glacial decay times at Richmond Gulf (RG) and Angerman River (AR) for an Earth model characterized by an upper mantle viscosity of 10^{21} Pa s and a lower mantle viscosity of 2×10^{21} Pa s, and a simplified (disk) ice load (dashed lines). Predictions are also shown for calculations modified to include an 80 km elastic lithosphere (solid lines) and the ICE–1 deglaciation history (dotted lines). (B) Post-glacial decay times computed using the viscosity profiles shown in Figs. 3A (solid line) and 3B (dotted line). The vertical bars on each frame represent the $\pm 1\sigma$ observational uncertainty.

ing history and a gravitationally self-consistent ocean load variation. The 'standard' ice model we adopt consists of a single disk load (elliptical in horizontal cross section and parabolic in vertical cross section) over each of Fennoscandia and Laurentia. Once again, a Monte Carlo procedure is used to determine decay times associated with the best-fitting form (1) through the numerical predictions. As an example, decay times computed using a viscosity model characterized by constant upper and lower mantle values of, respectively, 10^{21} and 2×10^{21} Pa s, with no lithosphere, are shown in Fig. 1a.

We also show, on Fig. 1a, predictions based on the same Earth model and the ICE–1 deglaciation chronology [Peltier and Andrews, 1976], as well as predictions generated using the standard ice model in combination with an Earth model having an 80 km elastic lithosphere (the sub-lithospheric viscosity variation is unaltered). These results confirm that the decay time parameterization provides, for the two sites considered here, a constraint on viscosity which is unbiased by uncertainties in the ice load history and lithospheric thickness.

Frechet kernels, which we denote by FK, provide a measure of the sensitivity of the decay time predictions to depth-dependent variations in radial viscosity profile, $\nu(r)$. In particular, we may write:

$$\delta \log \tau_i = \int_{CMB/a}^{1} FK_i[\nu(r); r]\delta \log \nu(r)\, dr , \quad (2)$$

where r is the radius (non–dimensionalized using the mean surface radius 'a'). Fig. 2 shows decay time kernels for the two sites considered in Fig. 1. The kernels are computed using the viscosity model considered in Fig. 1a (with no lithosphere; this model will henceforth be denoted 'TP', after the analysis of Tushingham and Peltier [1992]). The integrated area under the kernels in the lower and upper mantle obtain the ratios $\sim$ 2:1 and 1:2.5 for the Richmond Gulf and Angerman River predictions, respectively. This indicates that the Hudson Bay decay times, associated with the larger Laurentide ice sheet, are significantly more sensitive to lower mantle structure relative to upper mantle structure, than their counterparts in central Fennoscandia [see Mitrovica, 1996].

Mantle Convection and the Geoid

Our prediction of the non–hydrostatic geoid is based on the theory of buoyancy–induced flow in a spherical, self–gravitating, mantle that is assumed to be compressible [e.g., Forte and Peltier, 1991]. The relationship between the non–hydrostatic geoid and the density perturbations in the mantle that produce the flow may be expressed in terms of a kernel function G_ℓ as follows

$$N_\ell^m = \frac{3}{(2\ell + 1)\bar\rho} \int_b^a G_\ell[\nu(r)/\nu_o; r]\delta\rho_\ell^m(r)\, dr, \quad (3)$$

in which N_ℓ^m are the spherical harmonic coefficients (of degree ℓ and order m) of the non–hydrostatic geoid, $\bar\rho$ is the Earth's mean density, b is the mean radii of the core-mantle boundary (CMB), and $\delta\rho_\ell^m(r)$ are the radially–
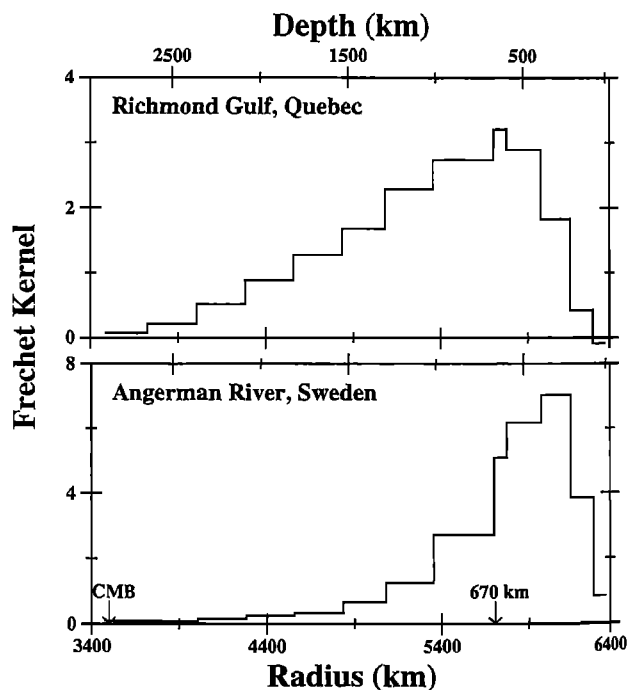

Fig. 2. Frechet kernels for the numerical prediction of the decay time associated with post-glacial RSL variations at Richmond Gulf and Angerman River. The calculations adopt the 'TP' viscosity profile given in Fig. 3a (dashed line).

varying harmonic coefficients of the density perturbations in the mantle. The geoid kernels G_ℓ are dependent on the depth variation of relative (dimensionless) viscosity $\nu(r)/\nu_o$, where ν_o is a reference scaling value, and hence the non–hydrostatic geoid is completely insensitive to the absolute value of mantle viscosity.

An essential ingredient in the mantle–flow modeling of the non–hydrostatic geoid is the velocity–density scaling coefficient $\delta \ln \rho / \delta \ln v$ which is needed to convert relative perturbations of seismic velocity $\delta v/v$ in the 3D mantle models into equivalent density perturbations $\delta \rho$ employed in (3). We employ the relative perturbations of seismic shear wave velocity $\delta v_S / v_S$ described by the model S.F1.K/WM13 of *Forte et al.* [1994]. The scaling coefficient $\delta \ln \rho / \delta \ln v_S$ for the mantle likely lies in the range $+0.1$ to $+0.4$ (see *Forte et al.* [1993]).

The non–hydrostatic geoid in the degree range $\ell = 2 - 8$) predicted using the TP viscosity model, and using $\delta \ln \rho / \delta \ln v_S = 0.4$, increases the variance to the corresponding geoid data by a factor of 22. In the case of $\delta \ln \rho / \delta \ln v_S = 0.1$, the variance increase is a factor of 1.2. In contrast, consider the relative viscosity profile $\nu(r)/\nu_o$ in Fig. 3b (note the right-hand axis). This model (henceforth 'FDW') is a 13–layer discretization of the profile inferred by *Forte et al.* [1993; Fig. 10c] on the basis of ($\ell = 2 - 8$) non–hydrostatic geoid data, and it yields (for a particular scaling coefficient profile) variance reductions of 85% to the geoid data and 81% to the corresponding free–air gravity anomalies.

Frechet kernels for the geoid harmonics (replace $\log \tau_i$ with N_l^m in 2), computed using the TP model, are not
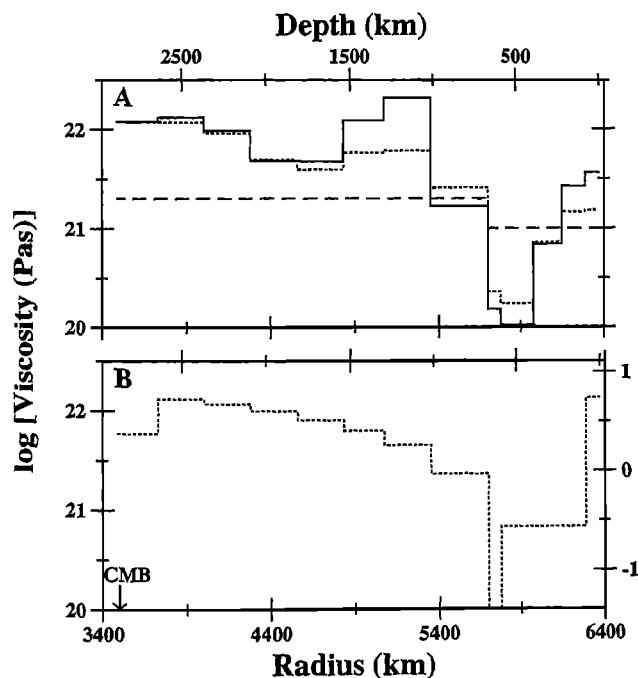

Fig. 3. Viscosity profiles discussed in the text. (A) The starting (dashed line) and final (solid line) models associated with our joint inversion of the convection observables and post–glacial decay time data. (B) The viscosity profile 'FDW' inferred by *Forte et al.* [1993]. In the *Forte et al.* [1993] analysis the absolute viscosity is unconstrained; the left axis on the figure refers to the scaling which provides a best–fit to the data set of post–glacial decay times.

shown here, but are similar to those appearing in *Forte et al.* [1993; Fig. 9]. The very-long-wavelength geoid is most sensitive to viscosity variations in the bottom of the upper mantle and in the bottom 1000 km of the lower mantle.

Inverse Calculations

In this section we adopt two approaches to finding models of mantle viscosity that satisfy both the GIA data and the non–hydrostatic geoid data. To begin, we search for a scaling viscosity ν_o such that the absolute viscosity $\nu(r)$ then delivered by the FDW relative viscosity profile best-fits the GIA decay time constraints. Using a large suite of forward calculations we have found that the scaling implied by the left-hand-axis of Fig. 3b minimizes the associated misfit. The fit of the model to the post-glacial decay times is evident from Fig. 1b.

Our second approach is to carry out a formal joint inversion of both the GIA and convection data sets. The full details of the inversion will be described elsewhere, however we note the following: (1) The inversions are parameterized in terms of $\log \nu(r)$ (and $\log \tau_i$) in a set of 13 layers extending from the CMB to the surface (as in Fig. 2); (2) we invert the harmonic coefficients of the long-wavelength free-air gravity anomaly, rather than the corresponding geoid harmonics; (3) we assume a scaling $\delta \ln \rho / \delta \ln v_S = 0.2$. Using other values (e.g., 0.4) has little effect on the inferred viscosity profiles and mainly effects the final misfit to the gravity data; (4) the non–linear, iterative, inversion is carried out using the 'Occam' algorithm [*Constable et al.*, 1987], and initiated using the TP model. We found that two iterations were necessary to produce convergence. (The second iteration did not significantly improve the fit to the decay time data; however, it was necessary to yield an acceptable fit to the free-air gravity harmonics.)

The results of the inversion are shown in Fig. 3a (solid line; the dotted line is the outcome of the first iteration). The model provides a variance reduction of 79% to the geoid data and 76% to the corresponding free-air gravity data. This gravity misfit is comparable to that provided by the FDW model. The decay times predicted using the model are shown in Fig. 1b.

The viscosity profiles inferred in this section (Fig. 3) suggest a significant viscosity increase, with depth, in the mantle. The viscosity in the bottom 1000 km of the lower mantle, which is constrained mainly by the convection observables, is near 10^{22} Pa s. Furthermore, the depth variation of the 'scaled' and inverted viscosity profiles within the upper mantle is quite similar to that inferred by others [e.g., *King and Masters*, 1992], particularly the strongly defined low–viscosity transition zone. A viscosity jump at 1000 km depth is evident in the inverted profile of Fig. 3a. Many analyses have suggested a seismic discontinuity at this depth [e.g., *Kawakatsu and Niu*, 1994]; however, while the results in Fig. 3a may be compelling in this regard, a viscosity jump at this depth does not appear to be unequivocally required (see Fig. 3b).

Mitrovica [1996] has shown that the *Haskell* [1935] constraint on mantle viscosity represents a weighted av-

erage across a region extending down to about 1400 km depth. The average, originally quoted in log space, has the range 20.90 ± 0.10 [*Mitrovica*, 1996]. Applying the Haskell resolving kernel to the profile of Fig. 3a, for example, yields a value of 20.88. *Mitrovica and Peltier* [1995] have argued that the decay times from Hudson Bay constrain the average viscosity within the depth range 400 to 1800 km to be near 2×10^{21} Pa s. The resolving kernel for this region, applied to the profile in Fig. 3a, yields a value of 1.9×10^{21} Pa s.

The origin of the observed free-air gravity anomaly over Canada has remained a matter of some debate. Within the degree range $l \leq 8$ the peak anomaly reaches a value of -28.5 mgals. We have found that the scaled viscosity model (Fig. 3b) yields a predicted peak anomaly of -30.0 mgals. 75% of this predicted signal (or -22.5 mgals) is due to mantle convection and the remainder is a GIA signal. The inverted viscosity model (solid line, Fig. 3a) produces a gravity anomaly of -26.5 mgals, with -16.5 mgals being contributed by mantle convection. We conclude that our new viscosity inferences reconcile the observed anomaly over Hudson Bay, and that this anomaly originates, in large part (but not exclusively), from the mantle convection circulation.

In a follow-up article we consider more fully the geophysical implications of our inferences and also present a joint inversion of a larger data base of GIA and convection observables (J.X. Mitrovica and A.M. Forte, submitted to *Journal of Geophysical Research*, 1996). The viscosity models we obtain are very similar to those in Fig. 3, although the absolute viscosity is slightly reduced, by a scaling of ~ 1.3, from those presented here.

References

Constable, S.C., R.L. Parker, and C.G. Constable, Occam's inversion: A practical algorithm for generating smooth models from electromagnetic sounding data, *Geophys.*, *52*, 289–300, 1987.

Forte, A. M., and W. R. Peltier, Viscous flow models of global geophysical observables, 1 Forward problems, *J. Geophys. Res.*, *96*, 20131–20159, 1991.

Forte, A. M., A. M. Dziewonski, and R. L. Woodward, Aspherical structure of the mantle, tectonic plate motions,

nonhydrostatic geoid, and topography of the core-mantle boundary, in *Dynamics of the Earth's Deep Interior and Earth Rotation, Geophys. Monogr. Ser.*, pp. 135–166, 72, ed. Le Mouël, J.-L., D. E. Smylie, and T. Herring, AGU, Washington, D.C., 1993.

Forte, A. M., R. L. Woodward, and A. M. Dziewonski, Joint inversions of seismic and geodynamic data for models of three-dimensional mantle heterogeneity, *J. Geophys. Res.*, *99*, 21,857–21,877, 1994.

Hager, B.H., Subducted slabs and the geoid: Constraints on mantle rheology and flow, *J. Geophys. Res.*, *89*, 6003–6015, 1984.

Haskell, N. A., The motion of a fluid under a surface load, 1, *Physics*, *6*, 265–269, 1935.

Kawakatsu, H., and F. Niu, Seismic evidence for a 920-km discontinuity in the mantle, *Nature*, *371*, 301–305, 1994.

King, S.D., and T.G. Masters, An inversion for the radial viscosity structure using seismic tomography, *Geophys. Res. Lett.*, *19*, 1551–1554, 1992.

Meier, M. F., Contribution of small glaciers to global sea level, *Science*, *226*, 1418–1421, 1984.

Mitrovica, J. X., Haskell [1935] revisited, *J. Geophys. Res.*, *101*, 555–569, 1996.

Mitrovica, J. X., and W. R. Peltier, Present-day secular variations in the zonal harmonics of the Earth's geopotential, *J. Geophys. Res.*, *98*, 4509–4526, 1993.

Mitrovica, J. X., and W. R. Peltier, Constraints on mantle viscosity based upon the inversion of post-glacial uplift data from the Hudson Bay region, *Geophys. J. Int.*, *122*, 353–377, 1995.

Nakada, M., and K. Lambeck, Late Pleistocene and Holocene sea-level change in the Australian region and mantle rheology, *Geophys. J. Int.*, *96*, 497–517, 1989.

Peltier, W. R., New constraint on transient lower mantle rheology and internal mantle buoyancy from glacial rebound data, *Nature*, *318*, 614–617, 1985.

Peltier, W. R., and J. T. Andrews, Glacial isostatic adjustment I. The forward problem, *Geophys. J. R. Astr. Soc.*, *46*, 605–646, 1976.

Richards, M. A., and B. H. Hager, Geoid anomalies in a dynamic Earth, *J. Geophys. Res.*, *89*, 5987–6002, 1984.

Sabadini, R., D. A. Yuen, and P. Gasperini, The effects of transient rheology on the interpretation of lower mantle rheology, *Geophys. Res. Lett.*, *12*, 361–365, 1985.

Tushingham, A. M., and W. R. Peltier, Validation of the ICE-3G model of Wurm-Wisconsin deglaciation using a global data base of relative sea level histories, *J. Geophys. Res.*, *97*, 3285–3304, 1992.

A. M. Forte, Institut de Physique du Globe de Paris, Dépt. de Sismologie, 4 Place Jussieu, Tour 24, 75252 Paris, Cedex 05, France.

J. X. Mitrovica, Dept. of Physics, University of Toronto, 60 St. George St., Toronto, Canada, M5S 1A7.